CHAPTER 65

THE MEASURED AND COMPUTED HOKKAIDO NANSEI-OKI EARTHQUAKE TSUNAMI OF 1993

Tomoyuki Takahashi¹, Nobuo Shuto¹ Fumihiko Imamura² and Hideo Matsutomi³

Abstract

The linear long-wave theory is used in the first stage to find the tsunami initial profile. The perfect reflection is assumed at the land boundary. On comparing the computed with the measured overall runup distribution, the best fault model is found among 24 models. It consists of three sub-faults dipping westward. It satisfies the measured land subsidence and overall distribution of runup heights in Okushiri Island.

Then, the shallow-water theory with bottom friction is used to simulate runup. The runup condition is used as the land boundary condition. The arrival time and runup heights agree well with the measured.

Introduction

At 22:17, July 12th, 1993, an earthquake of Ms=7.8 occurred off the southwestern coast of Hokkaido, in the Japan Sea. A giant tsunami was generated. It hit the island of Okushiri about 5 minutes after the earthquake, and claimed more than 200 lives. A big fire, caused by the tsunami, burned houses which were saved from the direct attack of the tsunami in Aonae, a small town at the southern end of Okushiri Island. The area of concern is shown in Fig.1 (Hokkaido Tsunami Survey Group, 1993).

Since the tsunami hit at night, its details could not be obtained from witnesses. The most reliable data would be the tsunami traces. Many parties were dispatched to

¹Disaster Control Research Center, Tohoku Univ., Sendai 980–77, Japan ²School of Civil Eng., Asian Inst. of Tech., G.P.O.Box 2754, Bangkok 10501 ³Dept. of Civil Eng., Akita Univ., Akita 010, Japan measure runup heights and collect such data as tide records. The authors also organized a survey team of 19 persons, and sent it to the site two days after the disaster. At the same time, the authors simulated the tsunami with the Harvard CMT solution. On exchanging results by faxs and phone calls between the survey team and the simulation team every morning and night, places and density of measurement points were determined. The authors considered that if there was a difference between the measured and the computed, this difference was really important to distinguish the special feature of the tsunami.

In the second section, tsunami data are shown and the special feature of this tsunami which should be satisfied by the simulation is summarized. In the third section, the method of simulation is briefly given. In the fourth section, initial profiles



Fig.1 Location of the area studied.

obtained from seismic data are shown and their defect are discussed. In the fifth section, a comparison is made between the measured tsunami runups and the simulated with the Harvard CMT solution. In the sixth section, a model of two sub-faults, DCRC-2, is proposed and examined. In the seventh section, a model of three sub-faults, DCRC-17a, is introduced. Among 24 models examined by the authors, the DCRC-17a model is considered the best at present. In the same section, the problems which requires a further study are also discussed.

Measured Runup Heights, Tide Records, Arrival Time and Ground Subsidence

Positions of aftershocks are shown in Fig.2 (Hokkaido Univ. et al, 1993). The vertical distribution of aftershocks in each section implies that it is very hard to determine the inclination angle of fault, which is closely related to the location of the crest of the initial tsunami profile. A reverse–slip fault dipping eastward (westward) makes the crest far from (near to) Hokkaido Island and results in a late (early) arrival of the tsunami.

Figure 3(a), (b) shows the measured runup heights in Okushiri Island and the mainland of Hokkaido. The highest runup of 31.7 m was obtained on the western shore of Okushiri Island directly facing the earthquake fault. It was found at the

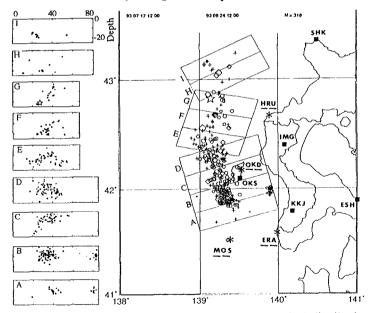


Fig.2 Distribution of aftershocks. Left figures are vertical distributions in the areas given by rectangles in the right figure.

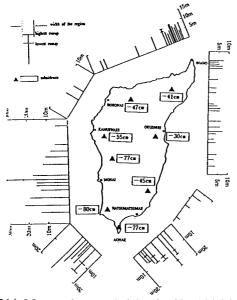


Fig.3(a) Measured runup heights in Okushiri island with the measured subsidence shown in rectangles.

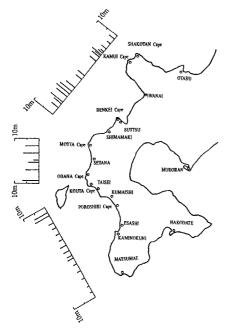


Fig.3(b) Measured runup heights in Hokkaido.

bottom of a tiny valley 50 m wide at its mouth on a pebble pocket beach 250 m long backed by cliffs. At the valley mouth and on the cliffs, runup heights were 22 m to 24 m. In order to simulate this high runup, very fine spatial grids (and, of course, very detailed maps) will be required.

Even on the eastern coast of Okushiri Island, high runup of 20 m was measured at Hamatsumae which is located in the sheltered area of Aonae Point. This may be a result of concentration due to refraction caused by the Okushiri Spur, a very wide shallow extending in the sea south of the point. In order to simulate the refraction effect, not only the detailed sea bottom contours but also the angle of tsunami incidence is important. This is closely related with the strike angle of the fault.

Along the eastern coast of Okushiri Island, runups show a wavy distribution, which implies the interaction of the tsunami entrapped around the island and the tsunami reflected from the mainland of Hokkaido.

Along the Hokkaido coast, tsunami runups are high from Taisei to Shimamaki and not high in the other region.

In the first column of Table 1, the arrival times collected from witnesses or determined from submerged clocks are summarized.

In Fig.3(a), the measured ground subsidence are also shown (Kumaki,Y. et al., 1993). Any fault model should yield the ground displacement coincident with them.

Method of Simulation

Two kinds of equations are used in the following simulation; the linear long-wave theory and the shallow-water theory with the bottom friction term included. The former is reduced to a set of difference equations, TUNAMI-N1, and the latter to TUNAMI-N2, by using the staggered leap-frog scheme. The details are given elsewhere (e.g., Shuto et al., 1986).

The area of simulation is from $138^{\circ}30$ 'E to $140^{\circ}33$ 'E and from $40^{\circ}31$ 'N to $43^{\circ}18$ 'N.

The initial tsunami profile is calculated with the Mansinha–Smylie method (1971) from fault parameters.

In simulations for modification and examination of fault models, TUNAMI-N1 is used with the perfect reflection condition at the land boundary. Overall agreements between the measured and computed are compared. The spatial grid is 450 m wide

Aonae	Aonae	Esashi	Taisei	Setana	Sukki	Shima-	Iwanai
(west)	(east)					maki	
4.5	4-5	11	5	5	3	5	15

Table 1 Arraival times

(unit:minute)

and the time step interval is 1 second.

TUNAMI-N2 is applied to the DCRC-17a model, selected as the best among 24 models. The spatial grids are varied; 450 m in Domain A, 150 m in Domain B and 50 m in Domain C. The runup condition is used at the land boundary,

Initial Profiles Proposed

Figure 4 compares tsunami initial profiles by different researchers and institutions. These profiles are obtained, based upon seismic data. Differences are resulted from the frequency range of seismic waves used in the analysis and from the locations of stations where the data were acquired.

With the accumulation of detailed and accurate seismic data, the situation became more and more complicated. No seismologists dare to determine what happened. Different from ordinary interplate earthquakes, no clear evidence was found about which plate is sinking below another. Almost a year later, many seismologists agree to think that the fault may dip westward.

Seismologists are now skeptical about the validity of vertical ground displacements which are calculated with such a method as the Mansinha–Smylie's. On contrary to the homogeneous displacement on the fault plane assumed in these methods, an actual fault motion is heterogeneous, and the resulted ground displacement is more complicated.

There is no other method and no other theory than the use of tsunami simulations, at present, to estimate the vertical displacement of sea bottom. One way is the tsunami inversion method introduced by Satake (1985), by which the initial profile is calculated back from tide records. The present paper uses another method, the trial-and-error repetition. We start the numerical tsunami simulation with an assumed initial profile, compare the simulated results with the measured runup heights to find the difference, modify the assumed initial profile, and repeat the procedure again.

When a tsunami model is determined, the number of faults is important. In the beginning, the authors used the Harvard CMT solution, which assumed a single fault. This model, however, could not simulate the tsunami well. Then, models of plural faults were examined. In this paper, one of two-fault models, DCRC-2, and one of three-fault models, DCRC-17a, are discussed.

Harvard CMT Solution

Immediately after the earthquake, seismic data seemed to support one of the Harvard CMT solution, the fault plane of which gently dipped eastward. Figure 5

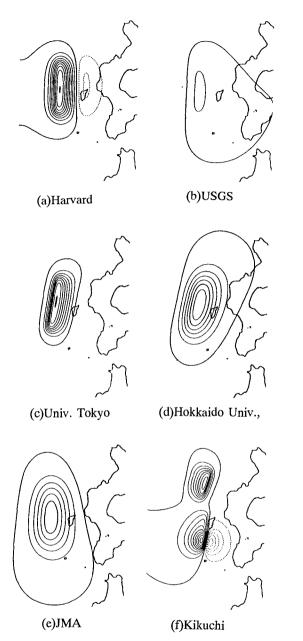


Fig.4 Proposed tsunami initial profiles. Solid lines are for upheaval and dotted lines for subsidence.

shows the vertical ground displacement (= tsunami initial profile) calculated for this solution. The crest is located at the western end of the tsunami source area.

With accumulation of seismic, geographical and tsunami data, differences of this model from the measured became non-negligible. Although this solution and the measured give the subsidence in Okushiri Island (Fig.6), the former gives the larger subsidence at the northern end of the island, while the latter reveals the larger subsidence of about 90 cm at the southern end.

The most important difference is found in the arrival time of tsunami. Every witnesses at Aonae confirm the fast arrival of the tsunami 4 to 5 minutes after the earthquake. The simulation, however, gives the arrival 7.5 minutes after the earthquake, as shown in Fig.7. In order to simulate this early arrival, the crest of tsunami initial profile should be located near the island; i.e., the fault should dip westward.

In Fig.8(a), (b), the computed runups are compared with the measured in Okushiri Island and Hokkaido. At Hamatsumae of Okushiri Island, the computed is too small. The same difference is found at Shimamaki of Hokkaido.

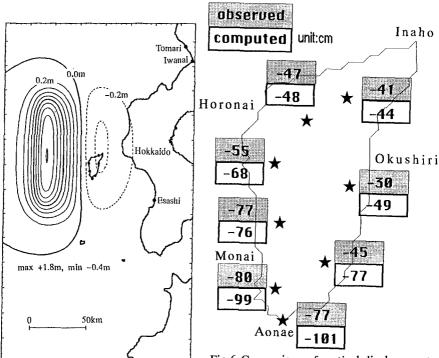


Fig.5 Tsunami initial profile computed for the Harvard CMT solution.

Fig.6 Comparison of vertical displacement in Okushiri Island between the measured and the computed with the Harvard CMT solution.

DCRC-2

Stimulated by the Kikuchi model (Fig.4 (f)), the authors assume plural faults. The first trial is DCRC-2, composed of two fault planes.

At the beginning of the modification, the authors take the following facts into consideration; aftershock distribution, ground subsidence in Okushiri Island and the witnessed arrival time of tsunami. The conclusion is that the faults must be reverse-slip faults inclining westward with a large dip angle.

Then, high runups at Hamatsumae is simulated. According to authors' assumption that these high runups are due to refraction, the strike direction of the south fault is adjusted because it governs the incident direction of the tsunami.

With these consideration, the initial profile for DCRC-2 is obtained as shown in Fig.9. Different from the Harvard CMT solution, there are two wave crests, both of which are located close to Okushiri Island. Contours are of more complicated shape.

The computed runups are compared with the measured in Fig.10. There are differences along the western coast. Along the south shore, the computed is much smaller than the measured, while the former is slightly smaller than the latter.

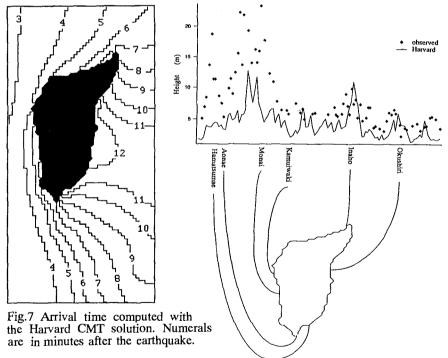


Fig.8(a) Comparison of runup heights between the computed with the Harvard CMT solution (solid line) and the measured (marks) along Okushiri Island.

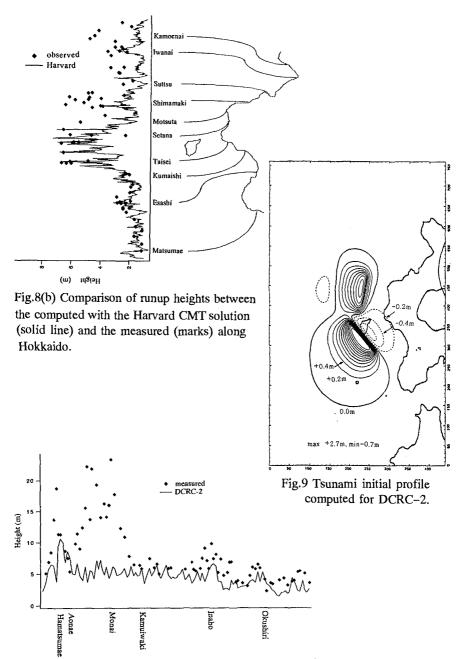


Fig.10 Comparison of runup heights between the computed with DCRC-2 (solid line) and the measured (marks) along Okushiri Island.

DCRC-17a

In order to solve the difference above mentioned, the authors divide the south fault into two faults with almost same strike directions. After several trials, DCRC-17a is found as the best. Its three fault planes are shown in Fig.11. The north fault is made longer than DCRC-2 in order to cover locations of aftershocks. Fault parameters are given in Table 2.

The initial profile of DCRC-17a is shown in Fig.12. The crest corresponding to the south sub-fault is 4.9 m high. Another crest is 2.2 m high, corresponding to the north sub-fault. The central fault does not yield any crest, because its slip is small.

The computed vertical displacement in Okushiri Island is compared with the measured in Fig.13. Compared to the Harvard CMT solution (see Fig.6), the agreement is much better.

Figure 14 shows the computed arrival time. The tsunami arrives at Aonae about five minutes after the earthquake, while it does 7.5 minutes in Fig.7 for the Harvard CMT solution.

Figure 15 compares runup height distributions around Okushiri Island. Overall agreement is fairly well, except for the neighborhood of Monai on the western coast, where the differences between the measured and the computed can only be explained by another simulation with very fine spatial grids as stated in the section of the measured runup heights. In order to evaluate the agreement, Aida's parameters, K and κ , the geometric mean of the ratio of the measured to the computed runup height and the corresponding variance, are used. For the whole island of Okushiri, K=1.048 and $\kappa = 1.469$. Distribution of K and κ for every coast is shown in Fig.16.

Figure 17 compares runup height distributions along Hokkaido. In the neighborhood of Esashi, the computed is higher than the measured. This indicates the need of a further modification. The initial tsunami height in the southern part of south fault should be made smaller than in the present model. In addition, a slight modification may be necessary to adjust the computed results near Suttsu and its neighborhood.

Fault	$M_0(\times 10^{27})$	depth	Strike(°)	Dip(°)	Slip(°)	Length	Wide	dislocation
North	3.85	10km	188	35	80	90km	25km	5.71m
Central	0.56	5km	175	60	105	30km	25km	2.50m
South	2.21	$5 \mathrm{km}$	163	60	105	24.5km	25km	12.00m
Total	6.62							

Table 2 Fault parameters of DCRC-17a.

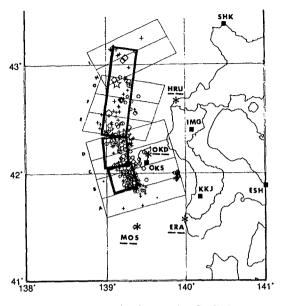


Fig.11 Three fault planes of DCRC-17a.

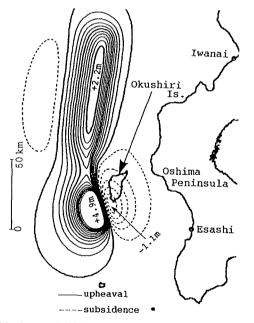
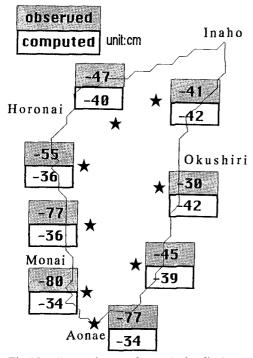


Fig.12 Tsunami initial profile computed for DCRC-17a.



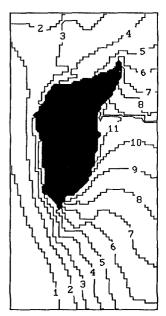


Fig.14 Arrival time computed with DCRC-17a. Numerals are in minutes after the earthquake.

Fig.13 Comparison of vertical displacement between the computed with DCRC-17a and the measured in Okushiri Island.

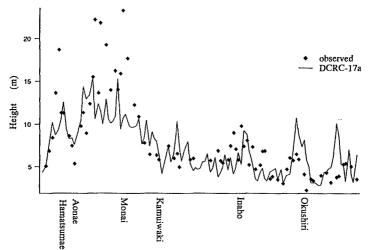


Fig.15 Comparison of runup heights between the computed with DCRC-17a (solid line) and the measured (marks) along Okushiri Island.

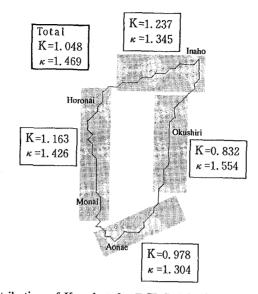


Fig.16 Distribution of K and κ for DCRC-17a along Okushiri Island.

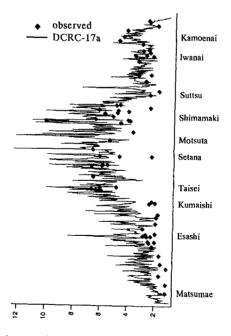


Fig.17 Comparison of runup heights between the computed with DCRC-17a (solid line) and the measured (marks) along Hokkaido.

Conclusions

In order to simulate the 1993 tsunami around Okushiri Island, the DCRC-17a model composed of three fault planes is obtained, by mostly adjusting the south and central faults. It satisfies the arrival time, runup distribution including high runups at Hamatsumae which is located in the sheltered area, and land subsidence.

In the present simulation, the maximum runup of 31.7 m in the neighborhood of Monai in Okushiri Island is not taken into consideration. A simulation with very fine spatial grids is required to simulate it.

Further adjustments of the south fault is necessary to explain the tsunami in the neighborhood of Esashi, Hokkaido. In addition, another adjustment is necessary for the northern part of the north fault. These adjustments may affect, to some extent, the wavy distribution of runup heights on the eastern coast of Okushiri Island, too.

References

Hokkaido Tsunami Survey Group:1993, Tsunami devastates Japanese coastal region, Eos, Transaction, AGU, 74, 417–432.

Mansinha, L. and Smylie, D.E.:1971, The displacement of the earthquake fault model, Bull. Seismol. Soc. America, 61, 1433–1400.

Satake, K.:1985, The mechanism of the 1983 Japan Sea earthquake as inferred from long period surface waves and tsunamis, Phys. Earth Planet. Interiors, 37, 249–260.

Satake, K. et al.:1988, Tide gauge response to tsunamis: Measurements at 40 tide gauge stations in Japan, J. Marine Res., 46, 557-571.

Shuto, N. et al.:1986, A study of numerical techniques on the tsunami propagation and run up, Science of Tsunami Hazard, 4, 111-124.